ACS Sustainable Chemistry & Engineering

pubs.acs.org/journal/ascecg

Research Article

Improved Reductive Catalytic Fractionation of Lignocellulosic Biomass through the Application of a Recyclable Magnetic Catalyst

Federico Bugli, Alessio Baldelli, Sam Thomas, Massimo Sgarzi, Matteo Gigli, Claudia Crestini, Fabrizio Cavani, and Tommaso Tabanelli*

Cite This: *ACS Sustainable Chem. Eng.* 2024, 12, 16638−16651

Read Online

ACCESS | Metrics & More | Article Recommendations | Supporting Information

ABSTRACT: The reductive catalytic fractionation (RCF) of second generation lignocellulosic biomass is an elegant one-pot process to obtain a highly delignified cellulose pulp, sugar-derived polyols, and depolymerized and stabilized lignin oils. However, the need of noble metal catalysts to prompt the reactions may impact the economic sustainability of the overall "lignin-first" biorefinery if the catalyst recovery and recyclability are not guaranteed. Herein, the use of a novel catalyst based on supported ruthenium over maghemite for the RCF of poplar sawdust is reported for the first time. This material allows us to obtain a pure cellulose pulp with a quantitative magnetic recovery efficiency after the first cycle. The obtained lignin oil is composed by a 12% yield in phenolic monomers (i.e., benzyl alcohol, 4-*n*-propylguaiacol, and 4-*n*-propylsyringol), together with dimers and trimers as confirmed by GPC analyses. The catalytic material was found to be stable and recyclable for three reaction cycles with only minor loss of RCF efficiency. On the other hand, the straightforward, lab-scale, magnetic recovery procedure needs to be further improved in the future to ensure quantitative recovery of the catalyst also after several RCF cycles.

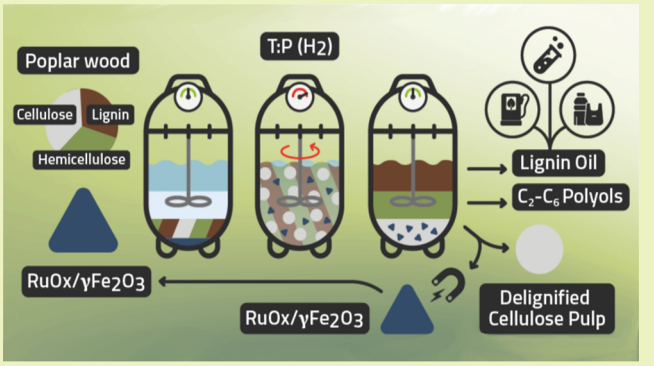

KEYWORDS: *biorefinery, reductive catalytic fractionation, lignocellulosic biomass, poplar, maghemite, magnetite, magnetic recovery*

1. INTRODUCTION

The search for sustainable alternatives to fossil-fuel-based productions has driven much attention from both academic and industrial research communities. This has led to the development of a relatively new integrated biorefinery concept aimed at the efficient valorization of second generation lignocellulosic biomass (LCB) as primary feedstock largely available worldwide.[1,2] The key constituents of LCB involve cellulose in a range of 35−50 wt %, hemicelluloses from 20 to 35 wt %, 5−30 wt % lignin, and other substances, such as ashes and others (i.e., waxes, terpenes, etc.), often referred to as "extractives" (1−10 wt %).[3] Despite several technologies that have already found industrial application, focusing especially on the valorization of the holocellulosic fraction (i.e., cellulose and hemicellulose), the fractionation processes currently employed for the isolation of the carbohydrate fractions suffers from several drawbacks, such as the need of harsh conditions, the use of strongly acidic or basic environment, the need of stoichiometric amount of toxic compounds and/or solvents, or the formation of inorganic waste.[4] As an example, in the kraft pulping process, a strong alkaline media (i.e., aqueous solution of NaOH and Na_2S, the so-called "white liquor") promotes biomass delignification through lignin solubilization, partial depolymerization, and repolymerization.[5] This is mainly due to the presence of HS^- ions, which improve the selectivity of the fractionation process without concurrently accelerating carbohydrate solubilization. Nonetheless, the harsh alkaline environment induces severe degradation and repolymerization reactions of the extracted lignin in the so-called "black liquor". This liquor is mostly incinerated to recuperate energy or undergoes consecutive acidification steps to promote the precipitation of a "kraft" lignin, characterized by both a contamination with sulfur and an irreparably altered structure, with an increased amount of new C−C linkages and branching at the expense of the more reactive ether bonds.[6] Conversely, the "native" lignin structure is mainly composed of phenolic monomers linked via ether bonds (mainly *β*-O-4′, *β*-5′, DBDO, and 5-O-4) and C−C bonds (*β*−*β*, 5−5′, *β*-5, and *β*-1′).[7,8] Among them, the *β*-O-4 is the most abundant linkage, which counts from 45 to 70% of the overall intermolecular bonds.[9] Luckily, this ether bond is the most easily cleaved and

Received: June 28, 2024
Revised: October 7, 2024
Accepted: October 8, 2024
Published: October 25, 2024

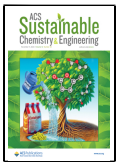

https://doi.org/10.1021/acssuschemeng.4c05299
ACS Sustainable Chem. Eng. 2024, 12, 16638−16651

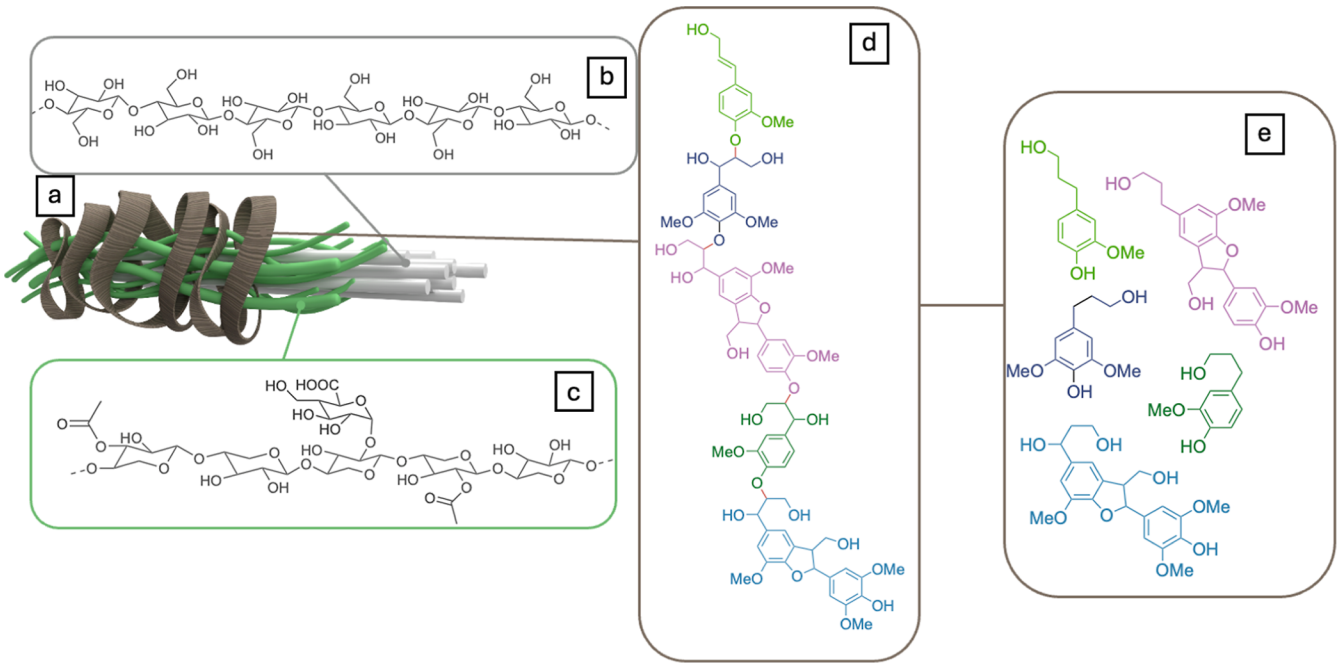

Figure 1. Schematic of LCB (a) fractionation in its main components: cellulose (b), hemicellulose (c), and lignin (d) and concomitant lignin depolymerization through β-O-4 catalytic ether bond cleavage toward monomeric and dimeric species (e).

therefore is the target of lignin depolymerization strategies, often tested on model molecules (i.e., 2-phenoxy-1-phenylethanol or 2-(2-methoxyphenoxy)-1-phenylethanol) instead of actual LCB. On the other hand, C−C bonds are much higher in energy, stable, and recalcitrant.[10,11] Therefore, harsh fractionation conditions may cleave those ether moieties and lead to irreversible repolymerization of the phenolic intermediates characterized by the presence of reactive functional groups such as aldehydes and double bonds, finally obtaining a recalcitrant technical lignin structure enriched in C−C bonds.[12,13] One possible solution could be to couple lignin extraction and depolymerization during the fractionation process with an in situ efficient stabilization of the obtained phenolic intermediates, thereby avoiding repolymerization routes and achieving the production of valuable phenolic compounds.[14] This approach could represent a key factor to promote a fully integrated biorefinery able to work synergistically with existing cellulose and hemicellulose facilities, thus valorizing every biomass component and reducing waste and costs.[15]

Following this strategy, an interesting approach is the reductive catalytic fractionation (RCF), first suggested in the 40s by Pepper and Hibbert for structural analysis of lignin,[16] and only since 2014 has it been reproposed for its potential as a biorefinery fractionation step.[17] In this process, the solubilization, depolymerization, and stabilization of lignin toward short oligomers and phenolic monomers are simultaneously accomplished through catalytic hydrogenation in the presence of a suitable solvent. The process' outcomes are, depending on the reaction conditions, a readily available carbohydrate pulp and a low MW lignin oil rich in phenolic monomers.[18] Typical RCF processes are performed in batch reactors at a temperature comprised between 180 and 250 °C for 2−6 h. Lignin extraction is aided by a polar protic solvent, while the reduction and hydrogenolysis of lignin-derived products is catalyzed by high H_2 pressure (10−60 bar) and redox catalysts.[17] Under these conditions, the β-O-4 bonds are cleaved and immediately stabilized through reduction. Previous scientific papers[12,18−20] investigated the RCF reaction and reached promising results in terms of aromatic monomer yield (up to 20−60%), delignification (up to ∼90%), and sugar retention in the pulp (up to 80−94%). A scheme of the depolymerization and stabilization process and of the main phenolics obtained by the RCF of LCB is shown in Figure 1.

Although these results seem to be remarkable, there is still plenty of room for improvement aimed at increasing the industrial attractivity of the overall process. In particular, a key factor is the catalyst recovery from the solid cellulosic pulp obtained during the fractionation process as well as catalyst stability and recyclability. Indeed, the most used catalysts are based on expensive noble metal active phases, particularly Ru, Pd, and Ni, supported on activated carbons or alumina.[17] Therefore, it is not surprising that the overall economics of the LCB biorefinery are deeply affected by the recovery efficiency of the heterogeneous catalyst after the reaction. The maximization of this parameter is indeed imperative not only to cut the costs of the noble metal makeup but also to produce a catalyst-free and more valuable cellulosic pulp, suitable for consecutive bio- and chemo-catalytic conversions. Several attempts aimed at optimization of the catalyst recovery efficiency are reported in the literature. For example, Renders et al. have worked with commercial Ru/C and Pd/C in the RCF of birch sawdust, reporting the possibility to recover these catalysts from the fibrous pulp through several solvent−solvent extractions with methanol-decane mixtures, finally obtaining a fine dispersion of the catalyst in the most apolar fraction.[21,22] However, the application of recovery techniques involving liquid−liquid extractions should take into account that slight variations in the carbon surface functionalization (e.g., carboxylic, phenolic, lactone, ether groups, and inorganic impurities) strongly affect the hydrophobicity of the material and consequently the efficacy of the partition in organic solvents.[23]

https://doi.org/10.1021/acssuschemeng.4c05299
ACS Sustainable Chem. Eng. 2024, 12, 16638−16651

Alternative engineering solutions to enhance catalyst recovery have been advanced through physical separation of the catalyst and the biomass. Schutyser et al.[24] suggested that the solvent under the applied conditions (i.e., methanol at high temperature and pressure) is almost entirely responsible for the extraction of lignin and its subsequent depolymerization through solvolytic β-O-4 bond cleavage forming unsaturated reactive intermediates such as coniferyl/sinapyl alcohol. Downsizing the catalyst role to the reduction and stabilization of highly reactive unsaturated oligomers and phenolic monomers, the use of catalyst pellets (commercial Ni/Al_2O_3) confined in a reactor basket (e.g., Carberry reactor) physically separated by the solid biomass can be justified, although diffusional limitations were reported to slow down the stabilization of intermediates, allowing higher occurrence of repolymerizations and reprecipitation.

On the same basis, other approaches are based on a semicontinuous RCF, foreseeing a first reactor with a fixed bed of LCB in which a continuous flow of hot solvent promotes lignin extraction before being collected in a second fixed bed reactor containing a noble metal catalyst and a reducing environment to promote the stabilization of the intermediates.[25] It should be noted that biomass must be unloaded and reloaded after every complete extraction cycle. Anderson et al.[26] provided kinetic studies on this semicontinuous (or decoupled) RCF isolating the limiting regimes of solvolysis and reduction, describing solvolysis as the rate-determining step in this approach. Specifically, what arises from this kinetic analysis could imply that β-O-4 bonds are not completely cleaved in the solvolysis step or that rearrangements of the intermediates could occur before their stabilization through catalytic reduction. Qiu et al.[27] investigated more in detail the impact of both the reaction conditions on lignin-derived compound repolymerization and the actual role of the catalysts in the process by adding the catalytic material at different times and temperatures in batch conditions. Ru/C catalyst was found to be unambiguously responsible for the reductive stabilization of unsaturated lignin while playing a minor role in depolymerization. At the same time, the immediate stabilization of the intermediates was found to be crucial to increase the monomers' yield, avoiding the condensation and precipitation of altered lignin. These parameters worsened when the catalyst was added as the reaction already reached 200 °C of the organosolv extraction. All of these results suggest the higher maturity of batch technologies for the RCF of LCB. Rinaldi and Ferrini[28] reported an RCF process catalyzed by Ni Raney, a bulk material magnetically recoverable from the processed pulp. The resulting pulps were demonstrated to have higher susceptibility to enzymatic hydrolysis because of their lower residual lignin content compared to those of the organosolv pulps.[29] However, more detailed results for catalyst recovery have not been reported. In addition, Ni-based catalysts are known to be susceptible to Ni leaching in similar reaction conditions.[25]

This urged us to consider the development of an innovative catalytic system based on noble metals supported over maghemite (i.e., RuO_x/γ-Fe_2O_3), not only active in the RCF process but also characterized by remarkable magnetic properties, thus allowing its separation and recovery from the fibrous cellulosic pulp through the application of an external magnetic field. Noteworthy, very little is known in the literature regarding the potentials related to the catalytic applications of supported noble metal over maghemite, and none ever reported their use for the target RCF processes.[30−34] Moreover, we decided to focus our attention on the fractionation of poplar wood sawdust, as one of the most spread hardwood species in Europe.[35,36]

2. EXPERIMENTAL SECTION

2.1. Raw Materials and Reagents. Solvents and reagents were supplied by Merck-Sigma-Aldrich and used as is. The detailed description of compounds and their purity can be found in Supporting Information, Chapter S1. Poplar wood was recovered by a local tree nursery, who gave us pruning remains of this plant species. The simple horseshoe magnet used for the magnetic recovery of the catalyst was supplied by Magnosphere (AlNiCo magnet, 30 × 20 × 20 mm, holds 4.5 kg).

2.2. Catalyst Preparation. RuO_x/γ-Fe_2O_3 was obtained by incipient wetness impregnation (IWI) of a commercial magnetite, Fe_3O_4 (Sigma-Aldrich, d < 50 nm, 98%) with a $RuCl_3 \times 3H_2O$ solution in ethanol followed by drying at 70 °C. The concentration of the solution was calculated to obtain a 5 wt % metallic Ru on the support. Finally, the powder was milled and calcined at 400 °C for 3 h (ramp 10 °C/min).

2.3. Catalyst Characterization. The powder X-ray diffraction (XRD) patterns were obtained with Ni-filtered Cu Kα radiation (λ = 1.54178 Å) on a Philips X'Pert vertical diffractometer equipped with a pulse height analyzer and a secondary curved graphite-crystal monochromator.

Nitrogen physisorption measurements were performed at −196 °C using an ASAP 2020 Micromeritics sorptiometer. The sample (∼100 mg) was outgassed at 40 mbar and 150 °C for 0.5 h and then heated at 250 °C for 0.5 h prior to the sorption experiment. The data were analyzed using standard BET and BJH methods.

The TPR, NH_3-TPD, and CO chemisorption experiments were carried out in an Autochem II (chemisorption analyzer, Micromeritics). In a typical TPR-O-R analysis, the calcined catalyst (∼0.1 g) was pretreated at 400 °C for 1 h under 30 mL min^{-1} of He. After the sample was cooled to 50 °C, the carrier gas was switched to 5% (v/v) H_2/Ar (30 mL min^{-1}), and the temperature of the catalyst was increased to 900 °C (10 °C min^{-1}) and held for 1 h. The signal was measured by means of a thermal conductivity detector. NH_3-TPD was performed as follows: ∼0.4 g of catalyst was loaded in a quartz reactor connected to the instrument and pretreated at 10 °C/min up to 450 °C for 1 h under 30 mL min^{-1} of He; then the sample was cooled to 100 °C, and the flow was switched to 30 mL min^{-1} of 10 mol % of NH_3 in He for 30 min. Weakly physisorbed ammonia was then removed by flowing He for 60 min at 100 °C. A TPD analysis was performed by reheating the sample at 10 °C/min up to 450 °C under He flow (30 mL min^{-1}), and the final temperature was kept for 1 h. CO chemisorption was performed over an in situ prereduced catalyst sample. 0.3 g of catalyst was first reduced by heating the sample up to 180 °C under 30 mL min^{-1} of 5 mol % of H_2 in He, and the final temperature was kept for 1 h. The reduced sample was then cooled to 40 °C, and pulses of 10 mol % of CO in He were repeated every 3 min until the full saturation of the sample was reached.

Ru content was measured by microwave plasma-atomic emission spectroscopy (MP-AES) analyses using an Agilent Technologies 4210 MP-AES instrument. In particular, for leaching tests, post-reaction solutions were filtered with a 0.2 μm Teflon syringe filter to completely and effectively remove the heterogeneous catalyst from the solution. Afterward, the obtained solution was diluted in H_2O to fall within the range of the calibration curve (0−300 ppm). The emission at 366.136 nm for Ru was evaluated, while for Fe, emissions at 373.713, 385.991, and 371.993 were considered. To verify Ru wt % amount on the synthesized catalyst, a precise amount of catalyst was completely mineralized in acid media, the solution was diluted, and emissions were evaluated as previously described.

Thermogravimetric analysis (TGA) of the spent catalyst was performed with a TA Instruments TGA 550 Discovery series. Typically, ca. 15 mg of sample was loaded inside the pan and then

https://doi.org/10.1021/acssuschemeng.4c05299
ACS Sustainable Chem. Eng. 2024, 12, 16638−16651

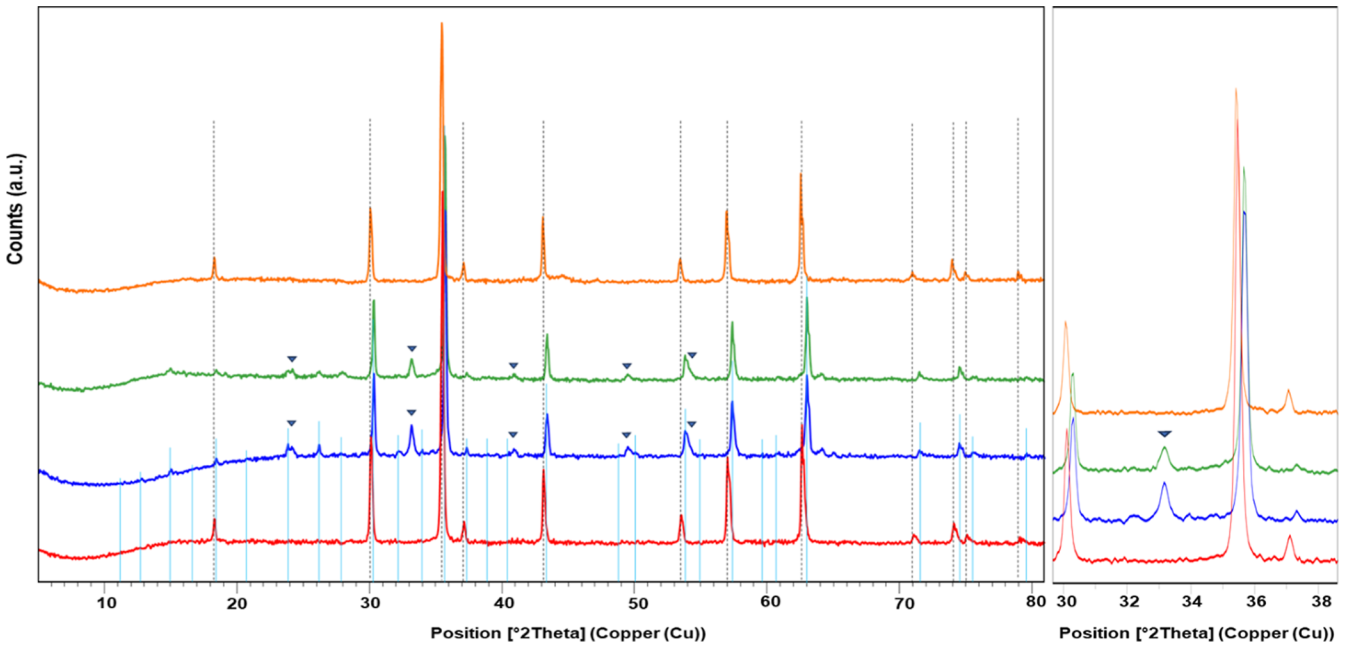

Figure 2. XRD diffraction patterns of pure magnetite (Fe_3O_4, in red), maghemite (γ-Fe_2O_3, in blue), fresh 5 wt % RuO_x/γ-Fe_2O_3 (green), and spent (after reaction) 5 wt % RuO_x/γ-Fe_2O_3 catalyst (orange). γ-Fe_2O_3 was obtained by calcining commercial magnetite at 400 °C for 3 h. Peaks related to magnetite (dotted black lines), peaks related to maghemite (full light blue lines), and hematite (blue triangles).

heated in a flux of 60 mL/min of either air or N_2 at 5 °C/min up to 720 °C.

Transmission electron microscopy (TEM) analyses were carried out using a TEM/STEM FEI TECNAI F20 microscope combined with energy-dispersive X-ray spectrometry (EDS) at 200 keV. A small amount of sample was suspended in ethanol and treated with ultrasound for 20 min. The suspension was deposited on a "multifoil-carbon film" sustained by a Cu grid and then dried at 100 °C. EDS was used to carry out elemental analysis. FEG-SEM TESCAN model MIRA3 equipped with a Bruker EDS Quantax 200/30 (30 mm^2 detector). The sample, in the form of dried powder, was displaced on a stub and kept in place with adhesive carbon tape. The observations and the maps were executed at 10 kV accelerating voltage and 2 nA beam current for a minimum of 10 min of acquisition time.

A PMC Micromag 2900 alternated gradient field magnetometer (AGM) (Lakeshore Cryotronics) was used to characterize the room temperature magnetic properties of the materials. Magnetization curves were obtained up to a maximum magnetic field of 12 kOe.

2.4. Reductive Catalytic Fractionation. In a typical RCF reaction, 1 g of lignocellulose, 0.1 g of catalyst, 20 mL of water, and 20 mL of 1-butanol were loaded in a 100 mL stainless steel batch reactor (AMAR Equipment). The reactor was flushed with N_2 and pressurized with 30 bar of H_2 at RT. The mixture was stirred at 750 rpm while the temperature was increased to 473 K, at which, typically, the pressure reached 50 bar, and the reaction started. After the reaction, the autoclave was rapidly cooled in an ice bath, and the pressure was gently released at RT. The reactor was then opened and washed with additional 100 mL water-butanol mixture (50% vol/50% vol), and the reactor solution was collected in a beaker (the detailed description of the magnetic separation procedure is reported in Chapter S3.2 in Supporting Information). After the magnetic separation, the reaction mixture was rapidly filtered to remove the carbohydrate pulp, while the filtrate solution was inserted in a separatory funnel in which spontaneous separation of the aqueous and organic phases occurred at RT. It is noteworthy that both depolymerized hemicellulose-derived products (polyols and short acids) and lignin-derived monomers and oligomers were mainly retained in the aqueous and organic phase, respectively. Samples of aqueous and organic phases were filtered using a 0.45 μm PTFE filter and kept for further characterizations. Subsequently, butanol was removed using a rotavapor, and the viscous brown oil obtained was dried at 60 °C overnight to calculate the weight of lignin-derived products and lignin first delignification efficiency (LFDE). The pulp was washed with ethanol to remove reaction mixture products adsorbed on the pulp surface, dried at 60 °C overnight, and weighted to calculate the overall LCB conversion. Conversion of LCB, LFDE, and catalyst recovery were calculated based on the equations reported in Supporting Information, Chapter S3. When the catalytic tests were performed with Ru/C powder, the recovery procedure of the catalyst was performed following a liquid–liquid extraction already reported in the literature.[21,22] Detailed procedures for catalyst recovery are reported in Supporting Information Section S3.2.

2.5. Determination of Structural Carbohydrates and Lignin in the Pristine Biomass and Post-RCF Pulps. Before characterization and reaction, pristine poplar wood samples were washed with water to remove soluble products (0.5 L for each gram of raw biomass). After being oven-dried overnight at 60 °C, the samples were processed through a ball milling procedure to reduce their size. In detail, 2 g of biomass was charged in a 60 mL stainless-steel reactor with 4 stainless-steel balls (2 characterized by a diameter of 12 mm and the other 2 of 6 mm), and the milling time was maintained at 10 min to not overheat the sample (and avoid degradation) and to only reduce the size of the LCB without affecting cellulose crystallinity. LCB was at this point sieved between 200 and 600 μm and stored in an open recipient for 24 h to reach equilibrium with air humidity. Both water and ash content in the ball-milled biomass were evaluated gravimetrically after specific thermal treatments following NREL procedures[36,37] (detailed information reported in Supporting Information, Section S4.1).

LCB was compositionally analyzed following a NREL LAP for standard biomass analysis[38] performing a concentrated 72 wt % H_2SO_4 hydrolysis for 1 h at RT, followed by dilute 4% H_2SO_4 hydrolysis in autoclave at 121 °C for 1 h. The abundance of structural components was calculated on data collected by HPLC analysis (for the holocellulosic components) and by gravimetric calculations for Klason lignin content following procedures and equations reported in Supporting Information Section S4.2.

2.6. Aqueous and Organic Phase Characterization. Aqueous phase solutions were analyzed through HPLC to quantitatively determine their composition (details in Supporting Information Section S5).

https://doi.org/10.1021/acssuschemeng.4c05299
ACS Sustainable Chem. Eng. 2024, 12, 16638−16651

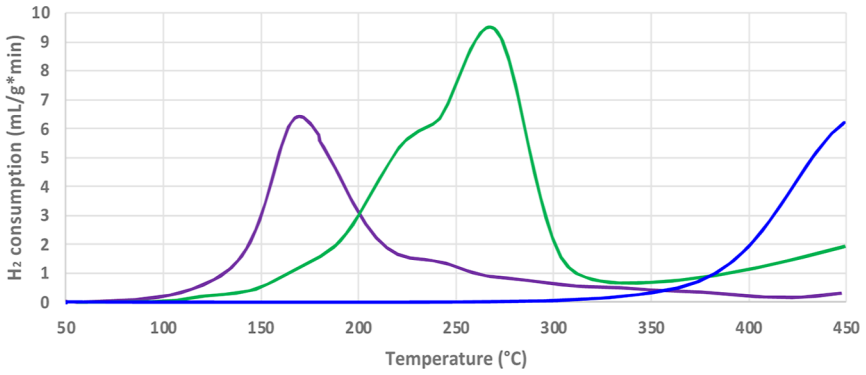

Figure 3. TPR profiles for the fresh 5 wt % RuO_x/γ-Fe_2O_3 (green), spent RuO_x/γ-Fe_2O_3 (purple), and γ-Fe_2O_3 (blue).

Organic phase solutions, sampled before rotary evaporation, were analyzed through GPC for a qualitative determination of the degree of depolymerization of lignin and lignin oligomers. To quantitatively determine the monomeric fraction derived from lignin depolymerization, a known amount of the organic phase was sampled from the overall solution and processed through a fractional distillation to quantitatively recover 1-butanol, which is recyclable for another RCF cycle by the distillation of (i) the 1-butanol-water azeotrope and (ii) the pure 1-butanol, thereby isolating a concentrated lignin oil. The oil was then processed via fractional precipitation using a mixture of toluene and *n*-heptane to promote the precipitation of the more polar oligomers and to obtain a solution containing only the lighter fraction of the lignin oil. This fraction was subsequently analyzed through GC−MS to confirm the monophenols' structures and quantitatively determine their abundance (detailed information can be found in Supporting Information Section S6).

3. RESULTS AND DISCUSSION

3.1. Catalyst Characterization. As stated above, only few works describe the possibility to synthesize and use noble metals supported over maghemite for application in catalysis.[31−34] Therefore, the characterization of the obtained material is described in detail. All the samples were prepared to contain a 5 wt % of reduced Ru^0 over the support to allow a direct comparison with a commercially available 5 wt % Ru/C. In particular, after the IWI of the ruthenium precursor onto the magnetite (Fe_3O_4), the calcination of the obtained material at 400 °C for 3 h leads to a complete transformation of the Fe_3O_4 support to a maghemite (γ-Fe_2O_3) phase (Figure 2), while $RuCl_3$ evolved toward oxide and hydrous oxide species.[38,39] During the transformation of Fe_3O_4 to γ-Fe_2O_3 the material preserves both the spinel crystal structure and the high magnetic properties. Chemically, only trivalent Fe ions are present in the obtained maghemite, as Fe^{II} positions are replaced by cation vacancies to guarantee charge neutrality of the cell with only a limited segregation of hematite.[41]

This implies that maghemite is characterized by a defective and smaller unit cell when compared to magnetite. The different lattice parameters lead to diffraction peaks shifted toward higher diffraction angles with respect to magnetite XRD patterns.[42] Figure 2 shows also the XRD patterns of the synthesized RuO_x/γ-Fe_2O_3 catalyst (not reduced, material obtained after the calcination at 400 °C) and a spent catalyst (after RCF process for 4 h at 200 °C). Interestingly, the fresh RuO_x/γ-Fe_2O_3 diffraction peaks are aligned to pure γ-Fe_2O_3 (ref code 01-076-1470, lattice parameters: 8.3279 and 8.3182 Å, respectively); after a reaction cycle, the diffraction peaks of the spent catalyst are aligned with those of pure Fe_3O_4 (ref code 01-088-0866, lattice parameters: 8.3623 and 8.3759 Å, respectively). As a matter of fact, the reductive environment of the RCF process and the spillover effect of the supported ruthenium facilitate the support reduction toward Fe_3O_4 (eq 1).

$$3\gamma\text{-}Fe_2O_3 + H_2 \rightarrow 2Fe_3O_4 + H_2O \quad (1)$$

Considering the stoichiometry of eq 1, if the reduction after the first reaction cycle is complete, the maximum recovery yield of the catalytic material will be equal to 96 wt % due to the weight loss expected from the reduction of the material. On the other hand, no Ru associated signals were detected on either the fresh or the spent catalysts. A possible explanation for this phenomenon is related to a very good dispersion of the Ru species on the catalyst surface. On the other hand, crystalline RuO_2 is reported to be formed at a higher calcination temperature (i.e., 550 °C), while hydrous ruthenium oxide species (HRO) are reported to be present at lower temperatures and are generally amorphous.[39,40] Moreover, it is reported in literature that the reduction toward Ru^0 of these HRO species $RuO_2 \times nH_2O$ takes place at lower temperatures than RuO_2; consequently, they are used as catalyst precursors for hydrogenation processes under milder conditions than those adopted in this work (i.e., 120 °C with 20 bar of H_2).[43] To better understand the reducibility of our materials, dedicated H_2-TPR analysis was performed over fresh RuO_x/γ-Fe_2O_3, spent RuO_x/γ-Fe_2O_3, and over nonimpregnated γ-Fe_2O_3 from 50 up to 450 °C (Figure 3).

The main reduction peak of γ-Fe_2O_3 to Fe_3O_4 is clearly visible in the fresh RuO_x/γ-Fe_2O_3 and γ-Fe_2O_3 samples, while further reduction peaks toward wüstite and metallic iron are not observed due to the relatively low final temperature selected for the analysis (i.e., 450 °C). Noteworthy, the main reduction peak is clearly shifted from 450 to 255 °C in the case of fresh RuO_x/γ-Fe_2O_3 due to the above-mentioned H_2 spillover effect promoted by the presence of Ru^0 that favors the reduction of the support. Moreover, the shoulder on the peak centered at a lower temperature, between 150 and 220 °C, represents the reduction of HRO species to Ru^0. This temperature range is in line with the conditions applied in our RCF process, thus confirming not only the possibility to activate (i.e., reduce) the ruthenium species during the catalytic tests without any need for additional pretreatment of the catalytic material but also to promote the progressive reduction of maghemite to magnetite. During this in situ coreduction of Ru species and the FeOx support, strong metal-support interactions may develop, potentially influencing the catalytic properties and stability of the system. The hydrogen consumption, related to the integration of the main reduction

https://doi.org/10.1021/acssuschemeng.4c05299
ACS Sustainable Chem. Eng. 2024, 12, 16638−16651

Table 1. Main Physical and Chemical Properties of the Catalytic Materials Obtained by (a) N_2 Physisorption, (b) MP-AES, and (c) TEM

	SSA (m^2/g)[a]	total pore volume (cm^3/g)[a]	micropore volume (cm^3/g)[a]	average pore diameter (nm)	Ru content (wt %)[b]	particle average dimension (nm)[c]
Ru/C	525	0.67	0.38	6	4.6	1.5
RuO_x/γ-Fe_2O_3	38	0.23	0	22	5.1	5−20

[a]N_2 physisorption. [b]MP-AES. [c]TEM.

peak, is equal to 0.0020 mol/g for γ-Fe_2O_3 and 0.0027 mol/g for fresh RuO_x/γ-Fe_2O_3. These values are in very good agreement with the stoichiometry for the reduction of maghemite to magnetite and eventually of RuO_2 to Ru^0 (see Table S2 in Supporting Information for details). On the other hand, the spent, after RCF, catalytic material shows a main reduction peak centered at 170 °C and a broad shoulder between 200 and 300 °C, corresponding to an overall H_2 consumption of 0.0018 mol/g. This value suggests not only a complete reoxidation of the metallic Ru to RuO_2 during the recovery of the catalyst after the reaction and its drying at 60 °C in air overnight (main reduction peak) but also a partial reoxidation of the magnetite to maghemite (Table S2). Despite these considerations on the nature of Ru species deposited on the magnetic support, Ru is deposited in low amounts (5 wt %), and the deposition technique usually takes place in the form of finely dispersed nanoparticles not visible through XRD analysis.[44] For this reason, dedicated TEM analyses were performed on both fresh Ru/C (Figure S6) and RuO_x/γ-Fe_2O_3 (Figure S7). As a matter of fact, the commercial Ru/C catalyst is characterized by a narrowed distribution of very small metallic Ru particles over the support with an average dimension of 1.5 nm, with few exceptions related to the presence of 8 to 11 nm particles of RuO_2. On the other hand, RuO_x/γ-Fe_2O_3 shows the presence of cubic ruthenium oxide particles dispersed over the support with a particle size between 5 and 20 nm.

Table 1 summarizes the characterization of the ad hoc synthesized RuO_x/γ-Fe_2O_3 and the commercial Ru/C in terms of specific surface area (SSA, m^2/g) and pore dimension (Figure S5), Ru content, analyzed through sample mineralization and MP-AES and ruthenium particle average dimension observed by TEM (Figures S6 and S7).

3.2. Magnetic RCF of Second Generation LCB. Figure 4 shows the structural composition of dried poplar wood

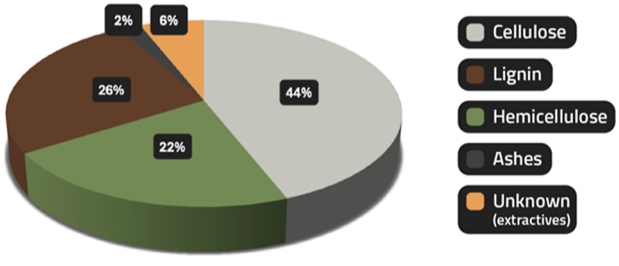

Figure 4. Structural composition of poplar sawdust.

obtained following the procedure reported in the Experimental Section.[38] Prior to this analysis and the catalytic tests, the raw biomass underwent only a washing step with water at RT (ca. 0.5 L/g), a mild drying step in an oven at 60 °C overnight, and a size reduction through a 10 min ball-milling treatment.

Noteworthy, in the great majority of the works related to RCF processes reported in literature, a further pretreatment step is foreseen for the extractives' removal to avoid the presence of nonstructural compounds that may limit the RCF efficiency or poison the catalytic system.[19,21,22,25] Indeed, especially when a certain biomass contains a high percentage (>10 wt %) of these compounds, a pre-extraction step is necessary to preserve the purity of the streams. Furthermore, the extracted compounds can be valorized vitamins, flavors, organic acids, and so forth.[45] On the other hand, a pre-extraction step would result in a further unitary operation to be foreseen in a process design that should be weighed carefully considering the economic viability and the scalability of the whole process. For this reason, considering the high percentage of structural components of poplar sawdust, close to 92 wt % on dry basis, the pre-extraction step was considered unnecessary for an effective fractionation of the biomass, thus reducing the operative units and enhancing the sustainability of the process.

The catalytic activity of the magnetic catalyst 5 wt % RuO_x/γ-Fe_2O_3 in the RCF reaction of poplar sawdust was first evaluated at 200 °C and 30 bar of H_2 and compared with a commercial 5 wt % Ru/C, the latter being a benchmark catalyst for the target reaction (Figure 5). A 50:50 binary mixture of 1-butanol and water was selected and used as reaction medium due to the advantages already described in the literature, namely, the good extraction efficiency toward lignin[43] and the capacity of 1-butanol to form two different phases with water once cooled again at RT.[21] Noteworthy, the lignin-derived products are retained in the organic fraction, while hemicellulose-derived products, e.g., polyols, are retained in the aqueous fraction. Water miscibility in the organic phase was checked after the reaction via a Karl Fischer titrator and was found equal to 20 wt % (see dedicated Section in Chapter S6 in Supporting Information). Moreover, a blank test was performed in the absence of any catalytic materials to better understand the actual role of the catalyst in the process.

In the literature, the catalyst role is reported to be more focused on the stabilization of lignin oligomers and on promoting the depolymerization of lignin fragments, while the lignin extraction and partial fractionation should proceed solvolytically.[19,27] This is in good agreement with our blank test results in which roughly 50% of the lignin is isolated in the organic phase as lignin oil, with this value being expressed as LFDE. It is foreseeable that the lignin oil is mainly composed of higher molecular weight lignin oligomers, which underwent partial recondensation due to the absence of a catalyst for the stabilization of the intermediates. This is supported by the poor yield in monophenolics, the partial delignification (due to the reprecipitation of technical lignin), and the GPC data (Table 2 and Figure S4), which confirm the presence of monolignol dimers and trimers. It is possible to note that the polydispersity value ($Đ$) of the sample treated with RuO_x/γ-Fe_2O_3 (3.1) is much lower than that of the blank (6.1), revealing higher stabilization of the intermediates, and slightly higher than the one treated with Ru/C (2.2), suggesting

https://doi.org/10.1021/acssuschemeng.4c05299
ACS Sustainable Chem. Eng. 2024, 12, 16638−16651

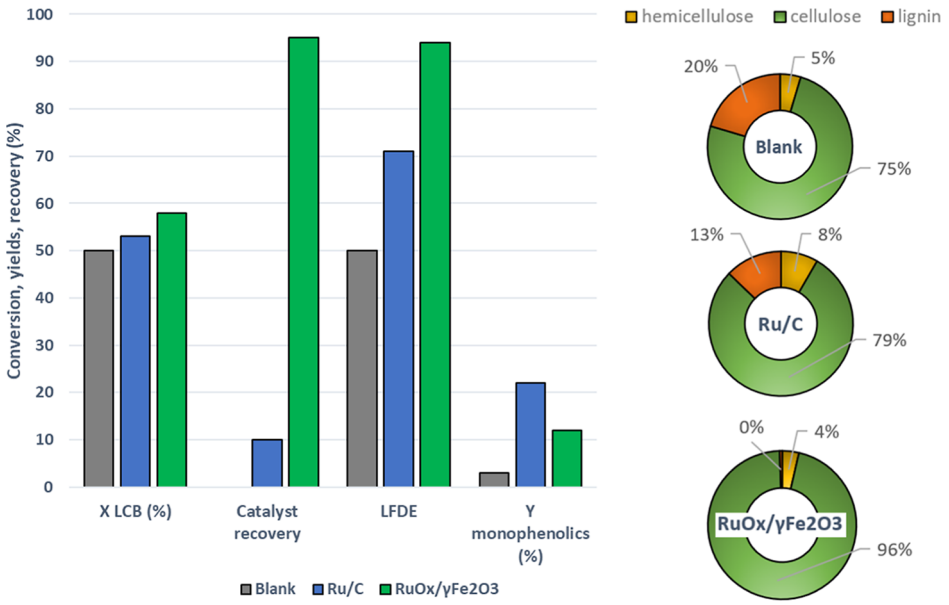

Figure 5. RCF results of poplar sawdust in terms of LCB conversion, catalyst recovery, LFDE, and monophenols yields obtained in the absence of any catalysts (blank sample) and in the presence of either Ru/C or $RuO_x/\gamma\text{-}Fe_2O_3$ (left). Structural composition of the obtained pulps (right). Reaction conditions: 200 °C, 4 h, catalyst/LCB = 10 wt %, solvent/LCB: 40 L/kg, and PH_2 (RT): 30 bar.

Table 2. GPC Data of Lignin Oils Obtained through the RCF of Poplar Sawdust in the Presence of Different Catalysts

	T (°C)	time (h)	PH_2 (bar)	M_n (g/mol)	M_w (g/mol)	$Đ$
blank	200	4	30	600	3700	6.1
Ru/C	200	4	30	500	1000	2.2
$RuO_x/\gamma\text{-}Fe_2O_3$	200	4	30	500	1600	3.1
$RuO_x/\gamma\text{-}Fe_2O_3$	200	2	30	700	2900	4.3

comparable performances in terms of degree of lignin depolymerization. On the other hand, the presence of a catalyst allows to greatly boost both the delignification (i.e., cellulose purity grade) and the monophenolics yield. Interestingly, Ru/C shows higher yields in monophenolics (up to 22%) but both LFDE and lignin conversion are lower compared to $RuO_x/\gamma\text{-}Fe_2O_3$.

The different physical and chemical properties of the supports lead to distinct catalytic behavior in the reaction environment. The Ru/C catalyst exhibits a significantly higher BET specific surface area (525 m^2/g compared to 38 m^2/g of $RuO_x/\gamma\text{-}Fe_2O_3$) due to the coexistence of both micro and mesopores (around 57% of total pore volume is derived from micropores, which contributes to the observed overall average pore diameter of 6 nm) and smaller Ru nanoparticles. On the other hand, $RuO_x/\gamma\text{-}Fe_2O_3$ is primarily characterized by meso- and macropores. This distinction in the pore size distribution plays a fundamental role in determining the catalytic performance. The predominantly microporous nature of Ru/C, while favoring efficient adsorption and depolymerization of smaller lignin oligomers (i.e., dimers), may create diffusional limitations for larger lignin fragments, particularly at the initial stages of the reaction when dealing with pristine biomass. In other words, considering a homogeneous distribution of Ru nanoparticles on the carbon surface, a considerable amount of Ru active centers, being confined in the micropores, will not be accessible to the larger lignin oligomers. This could explain the apparent contradiction between the enhanced Ru dispersion in Ru/C and its lower delignification efficiency (Table 2). On the other hand, the larger pores (meso and macro with an average pore diameter of 22 nm) in the structure of $\gamma\text{-}Fe_2O_3$, likely facilitates a more efficient interaction with the pristine biomass, the larger lignin fragments, and the catalyst surface. This could explain the higher delignification efficiency observed with $RuO_x/\gamma\text{-}Fe_2O_3$ despite its lower surface area and Ru nanoparticle dimensions and dispersion. The oxyphilic $\gamma\text{-}Fe_2O_3$ support may interact more effectively with the oxygen-rich lignin structure, leading to an enhanced interaction with the biomass. As a result, $RuO_x/\gamma\text{-}Fe_2O_3$ achieves a higher delignification efficiency, producing a highly pure cellulose pulp (with 99% lignin conversion) and a stabilized, yet poorly depolymerized, lignin oil (as confirmed by GPC analysis). The differences in pore structure and support chemistry between the two catalysts thus appear to be key factors in determining their performances in terms of delignification efficiency and lignin oil structure (higher monomer yields vs higher delignification with the formation of oils rich in stabilized oligomers).

In every catalytic test, hemicellulose is mostly depolymerized and converted to products readily solubilized in the aqueous phase; this fraction is known to undergo autohydrolysis in hydrothermal treatments due to the release of its acetyl side chains in form of acetic acid.[46] Indeed, in poplar samples, the presence of 3 wt % acetic acid with respect to the initial mass of lignocellulose was observed from the compositional analysis performed on pristine biomass and also found in the aqueous phase resulting from RCF process. The amount of acetic acid is enough to reach a final pH of ∼4.5 and an almost total dissolution of xylan polymer (see dedicated Section S5 in the Supporting Information related to aqueous phase HPLC analyses). On the contrary, cellulose retention in the pulp is close to unity for every RCF process, underlining the recalcitrance of the cellulose fraction to those mild acidic conditions, probably due to its high degree of crystallinity. As a matter of fact, the obtained cellulose pulp after RCF with

https://doi.org/10.1021/acssuschemeng.4c05299
ACS Sustainable Chem. Eng. 2024, 12, 16638−16651

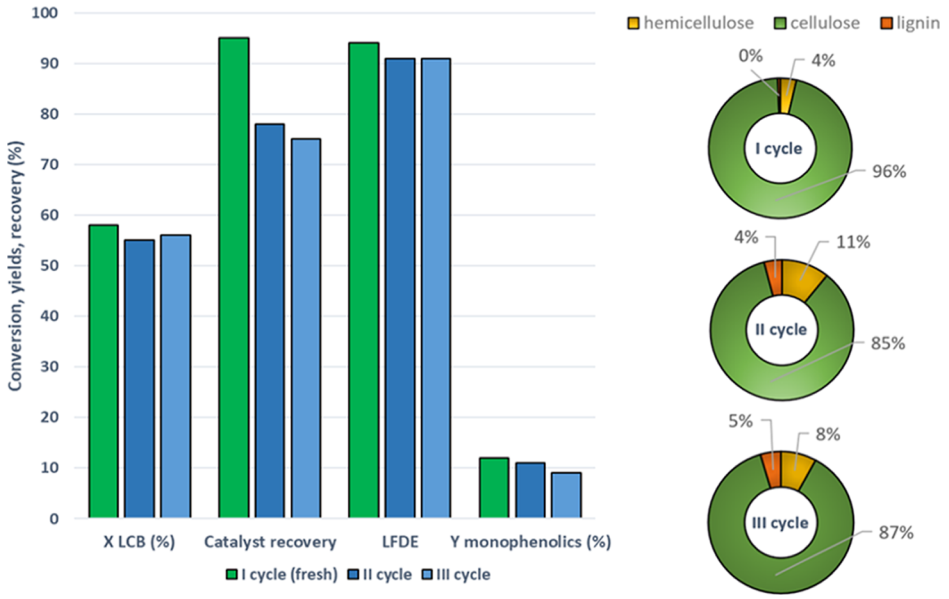

Figure 6. Recycling tests of RuO_x/γ-Fe_2O_3 catalyst in the RCF of poplar sawdust. LCB conversion, catalyst recovery, LFDE, and monophenols yields obtained (left). Structural composition of the obtained pulps (right). Reaction conditions: 200 °C, 4 h, catalyst/LC: 10 wt %, solvent/LC: 40 L/kg, and PH_2 (RT): 30 bar.

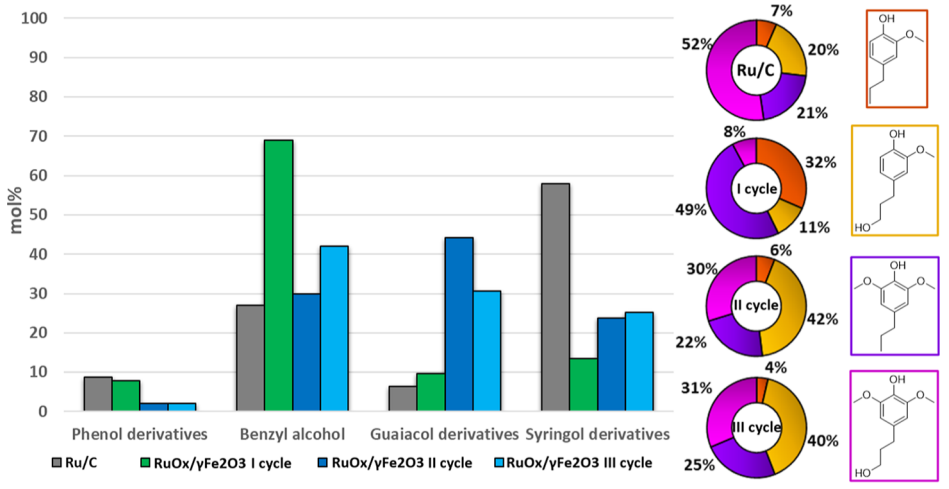

Figure 7. Molar distribution of the main monophenolic products obtained after the RCF of poplar sawdust in the presence of either Ru/C or RuO_x/γ-Fe_2O_3, fresh or recycled (left-hand side). The details on the guaiacyl and syringyl derivatives produced are reported on the right-hand side. 4-*n*-Propylguaiacol (orange), 4-*n*-propanolguaiacol (yellow), 4-*n*-propylsyringol (purple), and 4-*n*-propanolsyringol (pink). Reaction conditions: 200 °C, 4 h, catalyst/LC: 10 wt %, solvent/LC: 40 L/kg, and PH_2 (RT): 30 bar.

RuO_x/γ-Fe_2O_3 was characterized via XRD, clearly showing the typical crystalline pattern (Figure S3).

Additionally, another crucial difference between the two catalytic systems lies in their recovery efficiency and, therefore, recyclability (Figure 5). Specifically, liquid−liquid extraction procedures (e.g., using water and decane as solvents) are reported for the separation of carbon-supported catalysts from residual LC fibers and cellulose.[21,22] However, these protocols did not show good reproducibility. This finds an explanation considering that slight variations on the carbon surface functionalization (e.g., carboxylic, phenolic, lactone, ether groups, and inorganic impurities) strongly affect the hydrophobicity of the material and consequently the partition in organic solvents.[23] Supplemental separation techniques were applied to the pulps for the recycling of Ru/C catalyst (Supporting Information Section S3.2), but none of those techniques, even if employed together, gave results higher than 10 wt % catalyst recovery. Basically, most of the fine catalyst powders remain trapped inside the cellulose fiber network. On the contrary, the magnetic separation of RuO_x/γ-Fe_2O_3 led to remarkable results (95%) using a simple, lab-scale, and fast procedure (details reported in a dedicated chapter in the Supporting Information S3.2), which can certainly be further optimized in the future.

3.3. Catalyst Recyclability Tests and Trends in Monomer Production. On these bases, the recyclability of our catalyst was evaluated without any specific treatment or regeneration step between two different reactions (i.e., the recovered catalyst was only dried overnight at 60 °C). The obtained results are reported in Figure 6. Interestingly, only a slight decrement in LCB conversion, lignin extraction, or

https://doi.org/10.1021/acssuschemeng.4c05299
ACS Sustainable Chem. Eng. 2024, 12, 16638−16651

cellulose retention was observed after at least three consecutive RCF cycles.

A detailed analysis of the aromatic monomers obtained after the RCF process is reported in Figure 7. Surprisingly, while processing poplar wood sawdust, the main aromatic compound obtained was benzyl alcohol, together with the typically obtained monophenolic products, namely, 4-*n*-propylguaiacol/-syringol and 4-*n*-propanolguaiacol/-syringol.[17] Interestingly, benzyl alcohol was mainly obtained over the fresh RuO_x/γ-Fe_2O_3, together with 4-*n*-propylguaiacol and 4-*n*-propylsyringol, and even if guaiacols and syringols are widely reported to be formed during RCF, the formation of benzyl alcohol was, to the best of our knowledge, unprecedented.

Nevertheless, the formation of this compound could be easily associated with either the hydrogenolysis of benzyl alcohol esters units, which were reported to be contained in poplar's lignin structure, and/or from dissociations of benzyl alcohol-glycosides.[47,48]

The selectivity of the propyl-substituted compounds progressively declines with the recycle tests, favoring the formation of the corresponding propanol derivatives (Figure 7, right-hand side). This change in product distribution can be attributed to the gradual deactivation of weak and medium strength acid sites, which are present on the fresh RuO_x/γ-Fe_2O_3 catalyst surface (see NH_3-TPD, Figure S13, corresponding to overall acidity of 16 μmol NH_3/g, that is, an acid site density over the catalytic surface of about 0.42 μmol NH_3/m^2). Initially, these acid sites play a crucial role in fostering the dehydration of propanol derivatives to the corresponding propenyl chain, consecutively enhancing the production of the corresponding propyl phenolics via hydrogenation. However, as the catalyst undergoes multiple cycles without regeneration, organic compounds adsorb onto these acidic sites (as confirmed by TGA analysis, S9 in Supporting Information), diminishing their activity. Moreover, as shown by the FEG-SEM characterization of the spent material (Figure S8b), a progressive increase of the Ru nanoparticle dimension can be seen during the first cycles of reaction. All considered, the copresence of both acid sites over the support and of well-dispersed and active Ru nanoparticles is fundamental to foster the production of propyl-substituted phenolics. The product distribution observed in the case of fresh Ru/C further supports this hypothesis: the lack of acid sites on the carbon support means that Ru/C primarily catalyzes hydrogenation reactions without promoting the dehydration step, thus increasing the selectivity toward propanol substituted products, in particular, 4-*n*-propanolsyringol. Noteworthy, referring to the results shown in Figure 6 and bearing in mind that a complete reduction from RuO_x/γ-Fe_2O_3 to Ru/Fe_3O_4 during the first cycle led to a reduction of the catalyst mass of 4 wt %, the efficiency of the catalyst recovery declined from 95% (i.e., almost quantitative) after the first RCF cycle to ca. 78−75% in the following recycles. The reasons behind this drop were investigated in detail. In particular, MP-AES (Supporting Information Chapter S8) analyses were performed on both the aqueous and organic media after every RCF process, allowing us to exclude any leaching of either Ru or Fe in the organic phase, while only leaching corresponding to an average of 0.6% and 0.2% of the overall, initial amount of Fe and Ru, respectively, was found in the aqueous phase (Table S4). The missing amount of catalyst was successfully and quantitatively recovered; however, in the form of a mixture of α-Fe_2O_3 and γ-Fe_2O_3 (Figure S10), by performing the calcination of the obtained cellulose pulp at 575 °C for 3 h. This temperature was chosen according to the NREL procedures for the determination of ashes in LCB reported in Supporting Information (Section S4.1). Furthermore, it is known that the transition between maghemite and hematite starts to occur at annealing temperature above 550 °C, thus explaining the physical mixture of phases observed.[49] The reason that the recycled material is more easily trapped inside the cellulose pulp compared to the fresh material was attributed both to a progressive reduction of the particle size after few RCF cycles, probably due to damages promoted by the mechanical stirring during the reactions, and to the partial deposition of organic compounds over the catalyst surface, which decreased the magnetic susceptibility of the material. Indeed, Figure S9 shows the results obtained performing the TGA analyses on the spent Ru/Fe_3O_4 material after the third RCF cycle. The data clearly show the presence of adsorbed organic molecules (ca. 6.3 wt % loss) that desorb at around 300 °C in N_2 (Figure S9, top). On the other hand, the combustion in air of these compounds is favored at 255 °C. At this temperature, also the reoxidation of the material occurs, as demonstrated by both the slope change at ca. 290 °C and the lower mass loss (equal to 5.6 wt %, Figure S9, bottom). To further investigate the different magnetic behavior showed by the recycled catalyst, four selected samples were characterized by means of alternating gradient field magnetometry (AGM), namely, (1) maghemite (γ-Fe_2O_3), (2) fresh 5 wt % RuO_x/γ-Fe_2O_3, (3) spent 5 wt % RuO_x/γ-Fe_2O_3 catalyst after one reaction cycle, and (4) spent, recycled catalyst (i.e., after two reaction cycles). This way, the magnetic moment of the specimens as a function of the applied magnetic field was measured. Figure S12 reports the specific magnetization (per sample unit mass) of the different samples. Noteworthy, samples 1, 2, and 4 show very similar trends, with a magnetic saturation slightly above 50 emu/g, a value lower than the one reported for maghemite nanoparticles (i.e., 75 emu/g) as expected for granular materials mainly due to crystal disorder on the surface of the particles. On the other hand, sample 3 shows a higher maximum magnetization of 90 emu/g, this value being very close to the theoretical value of bulk magnetite. This can be explained by considering both TPR and XRD analyses. Indeed, while maghemite and fresh RuO_x/γ-Fe_2O_3 are expected to show the same behavior due to the same nature of the support, the behavior of the spent catalyst (sample 3) confirms the effective in situ reduction of the maghemite support toward the magnetite structure during the first RCF cycle (as confirmed by XRD, Figure 2) promoted by the presence of well-dispersed Ru nanoparticles over the support (Figures S7, S8a and Table S3). On the other hand, the loss of magnetic saturation observed for sample 4, to values closer to the pure maghemite, is worth of future investigation. As a preliminary hypothesis, this effect can be related to three main concurrent causes: (i) the partial reoxidation of magnetite to maghemite during the steps of recovery and drying of the catalyst after the reaction; (ii) the formation of bigger Ru particles over the surface of the spent material (observed in FEG-SEM figure S8b), which leads to an inefficient H_2 spillover effect during the reaction corresponding to an ineffective in situ reduction of the maghemite to magnetite; and (iii) the increased amount of adsorbed organic species compared to sample 3. All these factors might contribute to the ineffective catalyst recovery obtained after two reaction cycles. Nonetheless, future investigation will be required to fully understand and confirm

https://doi.org/10.1021/acssuschemeng.4c05299
ACS Sustainable Chem. Eng. 2024, 12, 16638−16651

this hypothesis. Finally, the qualitative shape of the magnetization curves indicates a small hysteresis of about 80 Oersted (0.8 mT), consistent with the presence of a small fraction of magnetic particles having size above 100 nm and which are not in the superparamagnetic state at room temperature.

All considered, the recovery efficiency of the recycled catalyst, a parameter of paramount importance to increase the economic sustainability of a lignocellulosic biorefinery based on RCF, could be improved in the future by optimizing the magnetic recovery step (i.e., by increasing the applied magnetic field) or by adding a suitable regeneration step for promoting the desorption/decomposition of the organic residues from the surface as well by designing more stable and efficient catalysts.

3.4. Preliminary Qualitative Environmental Considerations. To illustrate the innovative nature of the proposed research, the data obtained from this work are qualitatively compared to others reported in the literature. Few studies up to this point provided such specific evaluation on RCF.[50,51] Sels et al.[51] compared various RCF modalities, assessing their cost-effectiveness within a potential biorefinery process aimed at selling lignin oil and the enzymatic production of ethanol from cellulose pulp. By hypothesizing, as a first approximation, a specular macroscheme of a biorefinery, the conditions of this work can enhance different and significant technoeconomic parameters. At the current state of technology, there are only batch reactors for RCF that surpass laboratory scale,[18,52] making it necessary to focus on catalyst recovery. Herein, the magnetic nature of the catalyst would allow to avoid the need of multiple extraction steps and the waste of organic solvents reported for this operation at laboratory scale, such as *n*-decane.[22]

In terms of performance, our fresh RuO_x/γ-Fe_2O_3 catalyst exhibits a total delignification of cellulose pulp, obtaining up to 96 wt % purity of the pulp primarily composed of C6 sugars, while the remaining 4 wt % retains part of hemicellulose (i.e., C5 sugars). This would allow for better enzymatic treatment performance, in addition to a total recovery of cellulase enzyme, which, according to previous works, tends to irreversibly bind to lignin, inhibiting its activity and, most importantly, its recovery and reuse at the end of the process.[53,54] Regarding the use of solvents, in this work, we operated under typical laboratory conditions at 40 L/kg of processed biomass. Interestingly, we have found that, without significantly affecting the process performance (and especially the fluid dynamics in the reactor), this loading can be reduced to 20 L/kg with 10 bar of H_2 and 5 wt % of catalyst, probably lowering the monomer production but achieving almost complete delignification (Figure S11). This is also in line with the results obtained by Renders et al.[21] The 1-butanol-H_2O mixture allows an operating pressure of only 24 bar compared to the higher pressures reached using ethanol or methanol under the same conditions,[53] resulting in advantages in terms of safety and plant costs. Moreover, the use of 1-butanol-H_2O biphasic mixture also avoids an additional unit operation of the plant dedicated to the extraction of products derived from hemicellulose,[44] as opposed to working with monophasic mixtures.

Additionally, the solvent recovery was evaluated through fractional distillation on an actual post-reaction organic phase, mainly composed by 1-butanol, extracted lignin oil, phenolic monomers, and the soluble amount of water. Interestingly, the fractional distillation allowed the quantitative recovery of 1-butanol and of the dissolved water: first, by promoting the distillation of the 1-butanol-water azeotrope (weight fraction of water = 20.2%) at 89 °C, followed by the recovery of pure 1-butanol (the specific quantities are reported in the Supporting Information, Section S6.2). This process results in a concentrated lignin oil composed only of phenolic monomers, dimers, and trimers. Based on these data, a recovery system applicable to this reacting mixture is reported by Thoresen et al.,[55] where the azeotropic mixture can in any case be supplemented with fresh solvents, obtained at the end of the distillation columns, to reintegrate the starting mixture but also used for phase separation steps and eventual washings. Interestingly, by distilling the azeotropic mixture of 1-butanol and water, which is a minimum azeotrope, the energy costs related to this process may be lower compared with the distillation of the pure solvents.

Overall, this study presents innovative insights into the well-established RCF approach, offering qualitative comparisons with existing literature and pioneering the utilization of a magnetic catalyst as well as a novel catalyst separation technique for such processes in which the coproduction of a solid (fibrous cellulose pulp) may hinder the feasibility of other commonly applied methodologies. The activity of this catalyst enhances delignification even at milder operative pressure, which would facilitate further cellulose valorization due to the achieved high purity of the pulp. Furthermore, the contribution of different factors, namely, the proposed raw material (i.e., poplar sawdust), the binary solvent system, and the magnetic recovery of the catalyst, can minimize unit operations within the process, enhancing both the economic and environmental sustainability of the process.

3.5. Economic Evaluations and *E*-Factor Comparisons. From a general perspective, in most industrial chemical processes, the cost of the raw material contributes 40−70% of the cost of the final chemical product. Succeeding to valorize waste LCB (agricultural residues, pruning waste, etc.), obtainable at close to zero cost (or less than zero if contributions are obtained for their conversion and valorization), leads to many intrinsic advantages. The problem of valorizing these raw materials lies in their heterogeneity and chemical complexity. For this reason, a solid, efficient, and robust process is needed to unlock the full potential of this lignocellulosic biorefinery approach. Considering the chemical composition of poplar sawdust, with an almost negligible amount of extractives, its use as an RCF raw material would lead to the valorization of almost all of the incoming dry biomass. In the scientific literature, there are already several broad economic evaluations on the potential of the RCF process. In particular, Sels et al.[56] analyzed the productivity of the RCF process catalyzed by Ru/C (or Pd/C) considering 1 ton of birch sawdust (pretreated through boiling solvent extractions) as the raw material entering the process. Interestingly, they estimated an hydrogen consumption of only 3 kg (cost of H_2 estimated at €2.5/kg), obtaining (after 3 h of reaction at 30 bar of H_2 and 250 °C) 550 kg of carbohydrate pulp (i.e., a mixture of cellulose and hemicellulose), 100 kg of phenolic monomers (namely, 4-*n*-propylguaiacol, 4-*n*-propylsyringol, 4-*n*-propanolguaiacol, and 4-*n*-propanolsyringol), together with 75 kg of oligomers. To make the process cost-effective, Sels et al. consider the price of the lignocellulosic raw material variable between 50 and 100 €/ton and, considering processing subsequently the carbohydrate pulp obtained to produce sorbitol and xylitol (through a further hydrogenolysis in an acidic environment), estimate that

https://doi.org/10.1021/acssuschemeng.4c05299
ACS Sustainable Chem. Eng. 2024, 12, 16638−16651

Table 3. *E*-Factor Preliminary Evaluation[g]

entry	biomass type	dry lignocellulosic biomass IN (kg)	mass of products (kg)	mass of wastes produced in the different steps						*E*-factor
				H_2O (kg)	1-butanol (kg)	hemicellulose related byproducts (kg)	catalyst loss (kg)	additional solvents (kg)	extractives and ashes (kg)	
entry 1: this work	poplar sawdust	1	0.62	10	0.8[a]	0.2	0.004[c]	0	0.037	17.8
entry 2: ref 22	Eucalyptus	1	0.713	0	0.8[a]	0.17	0.02[d]	19[e]	0.034	28.1
entry 3: ref 21	birch sawdust	1	0.69	10	1.6[b]	0.2	0.03[d]	2[f]	0.025	20.1

[a]Conservative loss of 1-butanol estimated at a maximum of 10% (in fact, the recovery is close to quantitative). [b]Estimated loss of methanol due to degradation and methylation processes. [c]Actual loss of catalyst observed with the magnetic recovery. [d]Estimated Ru/C catalyst loss from the liquid−liquid extraction. [e]Boiling ethanol/toluene mixture required for the preliminary extraction of the biomass. [f]Estimated loss of solvents in the liquid−liquid extractions for catalyst recovery. [g]Products considered: sum of the mass of the cellulose pulp obtained and of lignin oil extracted. Note that the purity of the cellulose in the obtained pulp is not considered herein, but is a crucial point for further cellulose valorization processes.

they can obtain between 600 and 700 € from the sugar fraction. This alone represents an added value of 6−12 times the price of the raw material. The evaluation of the economic potential of lignin monomers and oligomers is not trivial. Nevertheless, it is possible to estimate an additional income of approximately 800 € for the sale of this fraction (for example, as alternative monomers for the synthesis of phenolic resins). Unfortunately, these assessments do not consider the actual noble-metal catalyst recovery efficiency and recyclability, as well as biomass pretreatments and plant operating costs (e.g., the cost of distillation/purification of the products). These detailed technoeconomic evaluations are complex and are not in the scope of this document.

We wish to underline the influence of the catalyst price on a hypothetical poplar sawdust-based, magnetic-catalyzed RCF biorefinery. For 1 ton of poplar sawdust (e.g., residues from carpentries, estimated price at 20 €/ton), we could obtain about 420 kg of pure cellulose, together with 200 kg of phenolic oil, composed by both monomers and oligomers. This shall require about 100 kg of 5 wt % RuO_x/γ-Fe_2O_3 catalyst, which costs at around 650 €/kg, with the appraised values for magnetite (≈15 €/kg) and ruthenium (≈12,780 €/kg) in various commercial platforms, namely, Ali Baba, Amazon, Inoxia, https://www.dailymetalprice.com/, etc. Thus, the cost per 100 kg of catalyst should be equal to approximately 65,300 €. Considering the prices of (i) 700−800 €/ton for good quality cellulose; (ii) 4.5 €/kg for the obtained phenolic compounds[57]; and (iii) a catalyst recovery efficiency of at least 98%, already taking into account the weight loss during the reduction of the precursor, once the recovery process is optimized starting from our simple lab-scale procedure, the following potential income per ton of processed biomass can be calculated (eq 2)

$$\begin{aligned}\text{income (€/ton)} &= \text{productsincome} - \text{rawbiomasscost} \\ &\quad - \text{reagent or catalyst depletion} \\ &= 420\ \text{kg} \times 0.8\ \text{€/kg} + 200\ \text{kg} \times 4.5 \\ &\quad \text{€/kg} - 1000\ \text{kg} \times 0.02 \\ &\quad \text{€/kg} - 3 \times 2.5\ \text{€/kg} - 65.3 \\ &\quad \text{€/kg} \times 100 \times 0.02 \\ &= -97.5\ \text{€/ton} \end{aligned} \quad (2)$$

The determined income reveals that catalyst cost dramatically affects the affordability of the process. From this calculation, a target recovery efficiency as high as 99% is mandatory to have a positive income (i.e., 555 €/ton of biomass processes). Notably, the Ru accounts for 97.8% of the overall cost of the catalyst, implying that the same considerations are mandatory also for the use of commercial 5 wt % Ru/C catalysts. In future works, catalysts with lower metal loading (i.e., 1 wt % of Ru) and better Ru dispersion will be utilized to enhance the economic sustainability of the processes. Additionally, it is not trivial to estimate the potential income of the hemicellulose-derived products. So, further evaluation must be made in the future to improve and promote the selective conversion of hemicellulose to xylitol in the aqueous phase, which would allow raising the profit margin (the market price of xylitol is between 1 and 2 €/kg).

Considering the preliminary quantitative environmental aspects, it must be kept in mind that a proper numeric comparison (i.e., for the calculation of the *E*-factor) is often not trivial. This is due to the lack of quantitative information on the streams (i.e., recovery efficiency of the catalytic system, solvents, waste, and byproduct formation) of the alternative processes reported in the literature. However, we decided to calculate our *E*-factor and compare it with those obtained and reported by Renders et al. in 2015[22] and 2018.[21] To do so, we must consider all the steps of a potential lignocellulosic biorefinery scheme, namely, (1) pre-extraction of raw lignocellulose with boiling solvents (entry 3, Table 3) or washing step with cold water and consecutive biomass drying (entries 1 and 3, Table 3); (2) size-reducing ball milling; (3) RCF process; (4) recovery of the cellulose pulp and the catalyst, where steps 2−4 are applied to all biomasses in Table 3; and (5) 1-butanol-H_2O phase separation and consecutive distillation (entries 1 and 3) or methanol distillation (entry 3). The obtained results normalized for 1 kg of dry LCB entering the reactor are reported in Table 3. All in all, the calculated *E*-factors are relatively similar to each other, as expected from very similar approaches. Nonetheless, the limitation of the number of operating units (i.e., avoid extractions with solvents) is crucial to lower the formation of wastes. Worthy of note, in the case of our approach (entry 1, Table 3), up to 90% of the calculated *E*-factor is related to the water used in the preliminary washing step of the poplar sawdust, a step which could be further optimized in the future.

https://doi.org/10.1021/acssuschemeng.4c05299
ACS Sustainable Chem. Eng. 2024, 12, 16638−16651

4. CONCLUSIONS

Herein, the use of a magnetic, easily recoverable, and recyclable supported ruthenium catalyst for the RCF of raw LCB is reported.

This represents a novel application of magnetic materials in the RCF process, serving as a proof of concept to enhance catalyst recoverability and process sustainability. Poplar sawdust was selected as a suitable raw material due to both its wide availability in Europe and the low amount of extractives. Indeed, compositional analysis have shown that roughly 92 wt % of the dry biomass is composed by structural components (lignin, cellulose, and hemicellulose), making this LCB suitable for a direct fractionation process, thus avoiding the need for preliminary extraction steps with boiling organic solvents aimed to the removal of nonstructural components, which may impact the overall process from an environmental and economic point of view. Interestingly, our RuO_x/γ-Fe_2O_3 precursor underwent an in situ reduction during the RCF process, yielding the active Ru/Fe_3O_4 phase without the need of any preactivation steps. This catalyst allowed us to obtain both a highly delignified cellulose pulp and a stabilized, but only partially depolymerized, lignin oil (monophenolic species yield equal to 12%). The high degree of delignification achieved demonstrates the potential of these magnetic catalysts for producing high-quality cellulose pulp, a key factor for industrial applications.

Among the monophenolic products obtained with the fresh catalyst, benzyl alcohol, 4-*n*-propylguaiacol, and 4-*n*-propylsyringol were the most abundant. Noteworthy, the catalytic system can be easily recovered by applying an external magnetic field with 95 wt % of recovery efficiency after the first cycle, a value outclassing the recovery efficiency of the benchmark Ru/C and highlighting the advantage of using magnetic materials in the process. On the other hand, by recycling the RuO_x/γ-Fe_2O_3, only a slight decline of the catalytic performances was observed. This was mainly linked to the partial fouling of the material with organic compounds, while a significant leaching of the active phase was excluded, proving the good stability of the material in the reaction environment. Nonetheless, a progressive lowering of the magnetic recovery efficiency was observed, a behavior that was linked to both the progressive reduction of the particle size after few RCF cycles, probably due to damages promoted by the mechanical stirring during the reaction, and the partial deposition of organic compounds over the catalyst surface, which decreased the magnetic susceptibility of the material. The recovery efficiency and the recyclability of the catalyst, pivotal for the actual sustainability and the economic feasibility of the entire process, could be easily improved in the future by optimizing the magnetic recovery step (i.e., by increasing the applied magnetic field) or by adding a suitable regeneration step to promote the desorption/decomposition of the organic residues from the catalyst surface.

In conclusion, this work serves as a proof of concept to demonstrate the potential of maghemite-supported materials in enhancing catalyst recovery, delignification efficiency, and overall process performance of the RCF. Future studies should focus on optimizing the used catalysts to improve their long-term stability, magnetic recoverability, and catalytic activity, potentially leading to more sustainable and economically viable biorefinery processes.

■ ASSOCIATED CONTENT

Supporting Information

The Supporting Information is available free of charge at https://pubs.acs.org/doi/10.1021/acssuschemeng.4c05299.

Details of experimental procedures, solid cellulose pulp and biomass analysis, GPC analysis of lignin oil, catalyst characterization (e.g., TPR, CO-chemisorption, NH_3-TPD, N_2 physisorption, TEM, FE-SEM, TGA of the spent catalytic material, XRD, and magnetization curves), and metal leaching analysis with MP-AES (PDF)

■ AUTHOR INFORMATION

Corresponding Author

Tommaso Tabanelli − *Dipartimento di Chimica Industriale "Toso Montanari", Università di Bologna, Bologna 40136, Italy; Center for Chemical Catalysis—C³, Alma Mater Studiorum Università di Bologna, Bologna 40136, Italy;* orcid.org/0000-0003-0616-8990; Email: tommaso.tabanelli@unibo.it

Authors

Federico Bugli − *Dipartimento di Chimica Industriale "Toso Montanari", Università di Bologna, Bologna 40136, Italy; Center for Chemical Catalysis—C³, Alma Mater Studiorum Università di Bologna, Bologna 40136, Italy*

Alessio Baldelli − *Dipartimento di Chimica Industriale "Toso Montanari", Università di Bologna, Bologna 40136, Italy*

Sam Thomas − *Dipartimento di Chimica Industriale "Toso Montanari", Università di Bologna, Bologna 40136, Italy*

Massimo Sgarzi − *Department of Molecular Sciences and Nanosystems, Ca' Foscari University of Venice, Venice 30172, Italy*

Matteo Gigli − *Department of Molecular Sciences and Nanosystems, Ca' Foscari University of Venice, Venice 30172, Italy;* orcid.org/0000-0003-3899-0399

Claudia Crestini − *Department of Molecular Sciences and Nanosystems, Ca' Foscari University of Venice, Venice 30172, Italy;* orcid.org/0000-0001-9903-2675

Fabrizio Cavani − *Dipartimento di Chimica Industriale "Toso Montanari", Università di Bologna, Bologna 40136, Italy; Center for Chemical Catalysis—C³, Alma Mater Studiorum Università di Bologna, Bologna 40136, Italy;* orcid.org/0000-0002-4282-6260

Complete contact information is available at: https://pubs.acs.org/10.1021/acssuschemeng.4c05299

Author Contributions

FB: investigation, data curation, conceptualization, and writing—original draft; AB: investigation, data curation; ST: manuscript review, characterization tests; MS: funding and validation, methodology, data curation, writing—review and editing; MG: methodology, data curation, writing—review and editing; CC: writing—review and editing: FC: writing—review and editing, TT: funding, conceptualization, methodology, writing—original draft.

Funding

Part of this work was financed by the European Union—NextGenerationEU through the Italian Ministry of University and Research under PNRR "Piano Nazionale di Ripresa e Resilienza"—Mission 4 "Istruzione e Ricerca" Component 2 "Dalla ricerca all'impresa", Investment 1.1, "Fondo per il

Programma Nazionale di Ricerca e Progetti di Rilevante Interesse Nazionale (PRIN)—Piano Nazionale di Ripresa e Resilienza, addressed to Progetti di Ricerca di Rilevante Interesse Nazionale". D.D. n. 104 del 2/2/2022, Project title: ENhanced CAtalytic fractionation and depolymerization Processes for a Straightforward valorization of lignocellULosic biomass to chemicals and mATErials (ENCAPSULATE) codice 2022KTAH2L—CUP: J53D23007620006. Part of this work was carried out within the Agritech National Research Center and received funding from the European Union Next-GenerationEU (PIANO NAZIONALE DI RIPRESA E RESILIENZA (PNRR)—MISSIONE 4 COMPONENTE 2, INVESTIMENTO 1.4—D.D. 1032 17/06/2022, CN00000022). This manuscript reflects only the authors' views and opinions, neither the European Union nor the European Commission can be considered responsible for them. MUR is also acknowledged for the Ph.D. grant of F.B. (Bando PON "Ricerca e Innovazione" 2014−2020).

Notes

The authors declare no competing financial interest.

■ ACKNOWLEDGMENTS

Reggi Pierluigi Falegnameria Artigiana Cotignola, Tabanelli Antonio, and Vivaio "I due riccioli verdi" di Greco Stefano are acknowledged for the poplar sawdust supplied.

■ ABBREVIATIONS

LBC, lignocellulosic biomass; RCF, reductive catalytic fractionation

■ REFERENCES

(1) Ragauskas, A. J.; Beckham, G. T.; Biddy, M. J.; Chandra, R.; Chen, F.; Davis, M. F.; Davison, B. H.; Dixon, R. A.; Gilna, P.; Keller, M.; Langan, P.; et al. Lignin valorization: improving lignin processing in the biorefinery. *Science* **2014**, *344* (6185), 1246843.

(2) Somerville, C.; Youngs, H.; Taylor, C.; Davis, S. C.; Long, S. P. Feedstocks for lignocellulosic biofuels. *Science* **2010**, *329* (5993), 790−792.

(3) Menon, V.; Rao, M. Trends in bioconversion of lignocellulose: biofuels, platform chemicals & biorefinery concept. *Prog. Energy Combust. Sci.* **2012**, *38* (4), 522−550.

(4) Kumar, R., Gaur, R., Raj, T., Kapoor, K. M., Satlewal, A., Prakash, G. R., Kumar, T. D. Method of pretreatment for enhanced enzymatic hydrolysis. U.S. Patent 10,487,347 B2, 2019.

(5) Argyropoulos, D. D.; Crestini, C.; Dahlstrand, C.; Furusjö, E.; Gioia, C.; Jedvert, K.; Henriksson, G.; Hulteberg, C.; Lawoko, M.; Pierrou, C.; Samec, J. S.; et al. Kraft Lignin: A Valuable, Sustainable Resource, Opportunities and Challenges. *ChemSusChem* **2023**, *16* (23), 202300492.

(6) Crestini, C.; Lange, H.; Sette, M.; Argyropoulos, D. S. On the structure of softwood kraft lignin. *Green Chem.* **2017**, *19* (17), 4104−4121.

(7) Crestini, C.; Melone, F.; Sette, M.; Saladino, R. Milled wood lignin: a linear oligomer. *Biomacromolecules* **2011**, *12* (11), 3928−3935.

(8) Sette, M.; Wechselberger, R.; Crestini, C. Elucidation of lignin structure by quantitative 2D NMR. *Chem.—Eur. J.* **2011**, *17* (34), 9529−9535.

(9) Crestini, C.; Crucianelli, M.; Orlandi, M.; Saladino, R. Oxidative strategies in lignin chemistry: A new environmental friendly approach for the functionalisation of lignin and lignocellulosic fibers. *Catal. Today* **2010**, *156* (1−2), 8−22.

(10) Liu, S.; Bai, L.; van Muyden, A. P.; Huang, Z.; Cui, X.; Fei, Z.; Li, X.; Hu, X.; Dyson, P. J. Oxidative cleavage of β-O-4 bonds in lignin model compounds with a single-atom Co catalyst. *Green Chem.* **2019**, *21* (8), 1974−1981.

(11) Lu, J.; Wang, M.; Zhang, X.; Heyden, A.; Wang, F. β-O-4 Bond Cleavage Mechanism for Lignin Model Compounds over Pd Catalysts Identified by Combination of First-Principles Calculations and Experiments. *ACS Catal.* **2016**, *6* (8), 5589−5598.

(12) Abu-Omar, M. M.; Barta, K.; Beckham, G. T.; Luterbacher, J. S.; Ralph, J.; Rinaldi, R.; Román-Leshkov, Y.; Samec, J. S.; Sels, B. F.; Wang, F. Guidelines for performing lignin-first biorefining. *Energy Environ. Sci.* **2021**, *14* (1), 262−292.

(13) Shuai, L.; Talebi Amiri, M.; Luterbacher, J. S. The influence of interunit carbon−carbon linkages during lignin upgrading. *Curr. Opin. Green Sustainable Chem.* **2016**, *2*, 59−63.

(14) Renders, T.; Van den Bosch, S.; Koelewijn, S. F.; Schutyser, W.; Sels, B. F. Lignin-first biomass fractionation: the advent of active stabilisation strategies. *Energy Environ. Sci.* **2017**, *10* (7), 1551−1557.

(15) Gigli, M.; Crestini, C. Fractionation of industrial lignins: opportunities and challenges. *Green Chem.* **2020**, *22* (15), 4722−4746.

(16) Pepper, J. M.; Hibbert, H. Studies on Lignin and Related Compounds. LXXXVII. High Pressure Hydrogenation of Maple Wood[1]. *J. Am. Chem. Soc.* **1948**, *70* (1), 67−71.

(17) Renders, T.; Van den Bossche, G.; Vangeel, T.; Van Aelst, K.; Sels, B. Reductive catalytic fractionation: state of the art of the lignin-first biorefinery. *Curr. Opin. Biotechnol.* **2019**, *56*, 193−201.

(18) Cooreman, E.; Vangeel, T.; Van Aelst, K.; Van Aelst, J.; Lauwaert, J.; Thybaut, J. W.; Van den Bosch, S.; Sels, B. F. Perspective on overcoming scale-up hurdles for the reductive catalytic fractionation of lignocellulose biomass. *Ind. Eng. Chem. Res.* **2020**, *59* (39), 17035−17045.

(19) Stone, M. L.; Anderson, E. M.; Meek, K. M.; Reed, M.; Katahira, R.; Chen, F.; Dixon, R. A.; Beckham, G. T.; Román-Leshkov, Y. Reductive catalytic fractionation of C-lignin. *ACS Sustainable Chem. Eng.* **2018**, *6* (9), 11211−11218.

(20) Vangeel, T.; Renders, T.; Van Aelst, K.; Cooreman, E.; Van den Bosch, S.; Van den Bossche, G.; Koelewijn, S. F.; Courtin, C. M.; Sels, B. F. Reductive catalytic fractionation of black locust bark. *Green Chem.* **2019**, *21* (21), 5841−5851.

(21) Renders, T.; Cooreman, E.; Van den Bosch, S.; Schutyser, W.; Koelewijn, S. F.; Vangeel, T.; Deneyer, A.; Van den Bossche, G.; Courtin, C. M.; Sels, B. F. Catalytic lignocellulose biorefining in n-butanol/water: a one-pot approach toward phenolics, polyols, and cellulose. *Green Chem.* **2018**, *20* (20), 4607−4619.

(22) Van den Bosch, S.; Schutyser, W.; Vanholme, R.; Driessen, T.; Koelewijn, S. F.; Renders, T.; De Meester, B.; Huijgen, W. J. J.; Dehaen, W.; Courtin, C. M.; Lagrain, B.; et al. Reductive lignocellulose fractionation into soluble lignin-derived phenolic monomers and dimers and processable carbohydrate pulps. *Energy Environ. Sci.* **2015**, *8* (6), 1748−1763.

(23) Bellè, A.; Tabanelli, T.; Fiorani, G.; Perosa, A.; Cavani, F.; Selva, M. A multiphase protocol for selective hydrogenation and reductive amination of levulinic acid with integrated catalyst recovery. *ChemSusChem* **2019**, *12* (14), 3343−3354.

(24) Van den Bosch, S.; Renders, T.; Kennis, S.; Koelewijn, S. F.; Van den Bossche, G.; Vangeel, T.; Deneyer, A.; Depuydt, D.; Courtin, C. M.; Thevelein, J. M.; Schutyser, W.; et al. Integrating lignin valorization and bio-ethanol production: on the role of Ni-Al 2 O 3 catalyst pellets during lignin-first fractionation. *Green Chem.* **2017**, *19* (14), 3313−3326.

(25) Anderson, E. M.; Stone, M. L.; Katahira, R.; Reed, M.; Beckham, G. T.; Román-Leshkov, Y. Flowthrough reductive catalytic fractionation of biomass. *Joule* **2017**, *1* (3), 613−622.

(26) Anderson, E. M.; Stone, M. L.; Hülsey, M. J.; Beckham, G. T.; Román-Leshkov, Y. Kinetic studies of lignin solvolysis and reduction by reductive catalytic fractionation decoupled in flow-through reactors. *ACS Sustainable Chem. Eng.* **2018**, *6* (6), 7951−7959.

(27) Qiu, S.; Wang, M.; Fang, Y.; Tan, T. Reductive catalytic fractionation of lignocellulose: when should the catalyst meet

https://doi.org/10.1021/acssuschemeng.4c05299
ACS Sustainable Chem. Eng. 2024, 12, 16638−16651

depolymerized lignin fragments? *Sustain. Energy Fuels* **2020**, *4* (11), 5588−5594.
(28) Ferrini, P.; Rinaldi, R. Catalytic biorefining of plant biomass to non-pyrolytic lignin bio-oil and carbohydrates through hydrogen transfer reactions. *Angew. Chem., Int. Ed.* **2014**, *53*, 8634−8639.
(29) Ferrini, P.; Rezende, C. A.; Rinaldi, R. Catalytic upstream biorefining through hydrogen transfer reactions: understanding the process from the pulp perspective. *ChemSusChem* **2016**, *9* (22), 3171−3180.
(30) Cooreman, E.; Nicolaï, T.; Arts, W.; Aelst, K. V.; Vangeel, T.; den Bosch, S. V.; Aelst, J. V.; Lagrain, B.; Thiele, K.; Thevelein, J.; Sels, B. F. The future biorefinery: the impact of upscaling the reductive catalytic fractionation of lignocellulose biomass on the quality of the lignin oil, carbohydrate products, and pulp. *ACS Sustainable Chem. Eng.* **2023**, *11* (14), 5440−5450.
(31) Behera, M.; Tiwari, N.; Basu, A.; Rekha Mishra, S.; Banerjee, S.; Chakrabortty, S.; Tripathy, S. K. Maghemite/ZnO nanocomposites: A highly efficient, reusable and non-noble metal catalyst for reduction of 4-nitrophenol. *Adv. Powder Technol.* **2021**, *32* (8), 2905−2915.
(32) Hajdu, V.; Prekob, A.; Muránszky, G.; Kocserha, I.; Kónya, Z.; Fiser, B.; Viskolcz, B.; Vanyorek, L. Catalytic activity of maghemite supported palladium catalyst in nitrobenzene hydrogenation. *React. Kinet., Mech. Catal.* **2020**, *129*, 107−116.
(33) Righi, G.; Magri, R. Surface reducibility, reactivity, and stability induced by noble metal modifications on theγ-Fe_2O_3maghemite (001) surfaces. *J. Phys.: Condens. Matter* **2020**, *32* (42), 425004.
(34) Jung, J.; Bae, S.; Lee, W. Nitrate reduction by maghemite supported Cu-Pd bimetallic catalyst. *Appl. Catal., B* **2012**, *127*, 148−158.
(35) Pisano, I.; Gottumukkala, L.; Hayes, D. J.; Leahy, J. J. Characterisation of Italian and Dutch forestry and agricultural residues for the applicability in the bio-based sector. *Ind. Crops Prod.* **2021**, *171*, 113857.
(36) Sluiter, A.; Ruiz, R.; Scarlata, C.; Sluiter, J.; Templeton, D. *Determination of Extractives in Biomass*, Laboratory Analytical Procedure (LAP), 2005; Vol. *1617*, pp 1−16.
(37) Sluiter, A.; B Hames, B.; Hyman, D.; Payne, C.; Ruiz, R.; Scarlatta, C.; Sluiter, J.; Templeton, D.; Wolfe, J. *Determination of Total Solids in Biomass and Total Dissolved Solids in Liquid Process Samples*, Laboratory Analytical Procedure (LAP) NREL/TP-510-42621, 2008; pp 1−6.
(38) Sluiter, A.; Hames, B.; Ruiz, R.; Scarlata, C.; Sluiter, J.; Templeton, D.; Crocker, D. *Determination of Structural Carbohydrates and Lignin in Biomass*, Laboratory analytical procedure, 2008; Vol. *1617*, pp 1−16.
(39) Gundekari, S.; Srinivasan, K. Hydrous ruthenium oxide: a new generation remarkable catalyst precursor for energy efficient and sustainable production of γ-valerolactone from levulinic acid in aqueous medium. *Appl. Catal., A* **2019**, *569*, 117−125.
(40) McKeown, D. A.; Hagans, P. L.; Carette, L. P.; Russell, A. E.; Swider, K. E.; Rolison, D. R. Structure of hydrous ruthenium oxides: implications for charge storage. *J. Phys. Chem. B* **1999**, *103* (23), 4825−4832.
(41) Shokrollahi, H. A review of the magnetic properties, synthesis methods and applications of maghemite. *J. Magn. Magn. Mater.* **2017**, *426*, 74−81.
(42) Nasrazadani, S.; Raman, A. The application of infrared spectroscopy to the study of rust systems-II. Study of cation deficiency in magnetite (Fe3O4) produced during its transformation to maghemite (γ-Fe2O3) and hematite (α-Fe2O3). *Corros. Sci.* **1993**, *34* (8), 1355−1365.
(43) Belluati, M.; Tabasso, S.; Bucciol, F.; Tabanelli, T.; Cavani, F.; Cravotto, G.; Manzoli, M. Sustainable isosorbide production by a neat one-pot MW-assisted catalytic glucose conversion. *Catal. Today* **2023**, *418*, 114086.
(44) Kawamata, Y.; Yoshikawa, T.; Koyama, Y.; Ishimaru, H.; Ohtsuki, S.; Fumoto, E.; Sato, S.; Nakasaka, Y.; Masuda, T. Uniqueness of biphasic organosolv treatment of soft-and hardwood using water/1-butanol co-solvent. *Ind. Crops Prod.* **2021**, *159*, 113078.
(45) Beatson, R. P. Chemicals from Extractives. *ACS Symp. Ser.* **2011**, *1067*, 279−297.
(46) Bassani, A.; Fiorentini, C.; Vadivel, V.; Moncalvo, A.; Spigno, G. Implementation of auto-hydrolysis process for the recovery of antioxidants and cellulose from wheat straw. *Appl. Sci.* **2020**, *10* (17), 6112.
(47) Devappa, R. K.; Rakshit, S. K.; Dekker, R. F. Potential of poplar bark phytochemicals as value-added co-products from the wood and cellulosic bioethanol industry. *BioEnergy Res.* **2015**, *8*, 1235−1251.
(48) Wang, Y.; Li, C.; Wang, Q.; Wang, H.; Duan, B.; Zhang, G. Environmental behaviors of phenolic acids dominated their rhizodeposition in boreal poplar plantation forest soils. *J. Soils Sediments* **2016**, *16*, 1858−1870.
(49) Jafari, A.; Shayesteh, S. F.; Salouti, M.; Boustani, K. Effect of annealing temperature on magnetic phase transition in Fe3O4 nanoparticles. *J. Magn. Magn. Mater.* **2015**, *379*, 305−312.
(50) Bartling, A. W.; Stone, M. L.; Hanes, R. J.; Bhatt, A.; Zhang, Y.; Biddy, M. J.; Davis, R.; Kruger, J. S.; Thornburg, N. E.; Luterbacher, J. S.; Rinaldi, R.; et al. Techno-economic analysis and life cycle assessment of a biorefinery utilizing reductive catalytic fractionation. *Energy Environ. Sci.* **2021**, *14* (8), 4147−4168.
(51) Arts, W.; Van Aelst, K.; Cooreman, E.; Van Aelst, J.; Van den Bosch, S.; Sels, B. F. Stepping away from purified solvents in reductive catalytic fractionation: a step forward towards a disruptive wood biorefinery process. *Energy Environ. Sci.* **2023**, *16* (6), 2518−2539.
(52) Feghali, E.; van de Pas, D. J.; Torr, K. M. Toward bio-based epoxy thermoset polymers from depolymerized native lignins produced at the pilot scale. *Biomacromolecules* **2020**, *21* (4), 1548−1559.
(53) Li, M.; Zhang, Q.; Chen, C.; Wang, S.; Min, D. Lignin interaction with cellulase during enzymatic hydrolysis. *Pap. Biomater.* **2019**, *4* (4), 15−30.
(54) Yang, B.; Wyman, C. E. BSA treatment to enhance enzymatic hydrolysis of cellulose in lignin containing substrates. *Biotechnol. Bioeng.* **2006**, *94* (4), 611−617.
(55) Thoresen, P. P.; Matsakas, L.; Rova, U.; Christakopoulos, P. Recent advances in organosolv fractionation: Towards biomass fractionation technology of the future. *Bioresour. Technol.* **2020**, *306*, 123189.
(56) Van den Bosch, S.; Schutyser, W.; Koelewijn, S. F.; Renders, T.; Courtin, C. M.; Sels, B. F. Tuning the lignin oil OH-content with Ru and Pd catalysts during lignin hydrogenolysis on birch wood. *Chem. Commun.* **2015**, *51* (67), 13158−13161.

https://doi.org/10.1021/acssuschemeng.4c05299
ACS Sustainable Chem. Eng. 2024, 12, 16638−16651